

# Model-based Development of Future Small EVs using Modelica

Yutaka Hirano    Shintaro Inoue    Junya Ota  
 Toyota Motor Corporation, Future Project Division  
 1200 Mishuku, Susono, Shizuoka, 410-1193 JAPAN  
 {yutaka\_hirano, shintaro\_inoue\_aa, junya\_ota}@mail.toyota.co.jp

## Abstract

To cope with demands for future low carbon society, development of new-type small electric vehicles (EVs) becomes very active. To reduce the energy consumption in various actual driving conditions, considering overall running resistance such as aerodynamic resistance, tire rolling resistance including cornering drag, mechanical and electrical losses, etc. will be necessary. On the other hand, to cope with reduced stability against external disturbances such as side wind because of the light weight, it was clarified that additional control of direct yaw moment is effective. In this paper, model-based development of a new electric vehicle using Modelica is described. Full vehicle model considering both vehicle dynamics and energy consumption was developed and utilized to investigate the best possible solutions for both basic design of the vehicle and design of the control system.

*Keywords: Future electric vehicles; Stability and Handling Performance; Energy Consumption*

## 1 Introduction

To cope with future mobility society, development of many new concept vehicles is increasingly active in recent years. Figure 1 shows a new EU regulation about light weight vehicles [1]. Those vehicles have characteristics of smaller size, lighter weight, less number of passengers than conventional vehicles. Also those vehicles tend to be equipped with lower RRC (Rolling Resistance Coefficients) tires and new driving systems mainly using electric motors to achieve less emission and less energy consumption. On the other hand, Toyota has a vision about future eco-cars as shown in Figure 2. Toyota thinks EVs are

suitable as short-distance mobility though there is a possibility of extending the driving range using range extender devices such as small combustion engine, additional battery and so on. In this paper, model-based-development of a new vehicle using Modelica is described. The models were developed based on Vehicle Dynamics Library (VDL) of Dymola.





Category & Category Name	Sub category & Sub category name	Example
L6e, Light quadricycle	L6Ae Light on-road quad	
	L6Be Light mini-car	
L7e, Heavy quadricycle	L7Ae Heavy on-road quad	
	L7Be Heavy mini-car	

Figure 1: New EU Regulation "Light-category vehicles" [1]

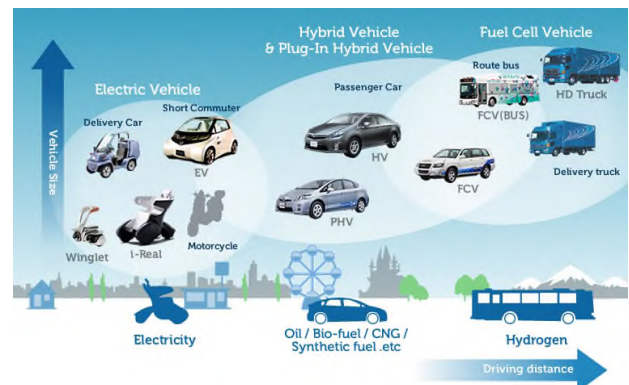


Figure 2: Toyota's scenario about future eco-cars

## 2 Modeling and simulation studies of the future vehicle

### 2.1 Target vehicle

Table 1: Specifications of the target vehicle

	Target plan	L7Be
Vehicle weight	< 600 kg	< 400* kg
Passengers	4	2
Max. Payload incl. passengers	300 kg	200 kg
Rated power	25 kW	< 15 kW
Max. speed	120 km/h	> 45 km/h
Driving range	> 100 km	-

(\* weight without batteries)

Table 1 shows comparison of specifications between our plan and EU regulation L7Be. Our aim is to develop a heavier and more powerful vehicle with more passengers than L7Be considering actual usefulness.

### 2.2 Simulation studies about basic specifications

To consider energy consumption, handling, stability, ride comfort and NVH (noise, vibration, harshness) performances of holistic vehicle, a full-vehicle model including mechanics, electronics, vehicle dynamics and control was made using Dymola. Moreover, a model of a new drive train system such as torque vectoring differential gear was developed and connected into the full-vehicle model. Figure 3 shows an example of the full-vehicle model. Details of the model will be explained later.

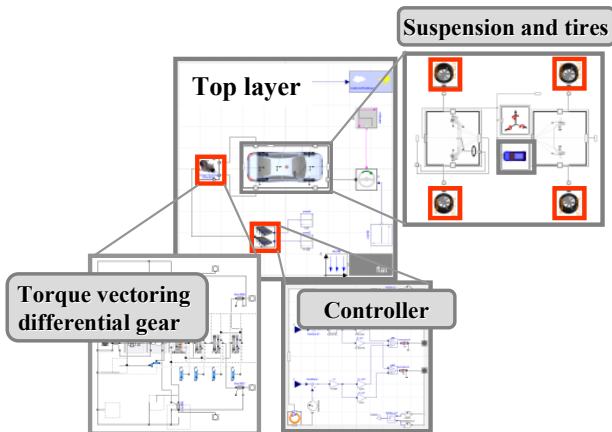


Figure 3: An example of full-vehicle model

Power consumption of each system was calculated simultaneously and was used for the investigation of good balance of energy consumption and vehicle performances. At first, total power of resistances acting on the vehicle was calculated by following equations [2].

Total resistance power:

$$P_v = P_{rr} + P_{ar} + P_{sy} + P_{sx} \quad (1)$$

Rolling resistance power:

$$P_{rr} = \mu_r mg \times V \quad (2)$$

Aerodynamic resistance power:

$$P_{ar} = \rho AC_D V^2 / 2 \times V \quad (3)$$

Cornering resistance power:

$$P_{sy} = \left[ \left( \frac{d_f}{C_{pf}} + \frac{d_r}{C_{pr}} \right) \times mA_y^2 / g \right] \times V$$

$$\approx \left[ \left( \frac{1}{C_p} \right) \times mA_y^2 / g \right] \times V \quad (4)$$

Longitudinal resistance power:

$$P_{sx} = (mA_x + mg \sin \theta) \times V \quad (5)$$

Here

$\mu_r$ : rolling resistance coefficient (RRC),

$g$ : acceleration of gravity [ $m/s^2$ ],

$m$ : vehicle mass [kg],

$V$ : vehicle speed [m/s],

$\rho$ : air density [ $kg/m^3$ ],

$A$ : vehicle frontal area [ $m^2$ ],

$C_D$ : aerodynamic resistance coefficient,

$d_f$ : front weight distribution ratio,

$d_r$ : rear weight distribution ratio,

$C_{pf}$ : front normalized cornering power [1/rad],

$C_{pr}$ : rear normalized cornering power [1/rad],

$C_p$ : average normalized cornering power [1/rad],

$A_y$ : lateral acceleration [ $m/s^2$ ],

$A_x$ : longitudinal acceleration [ $m/s^2$ ],

$\theta$ : road inclination [rad].

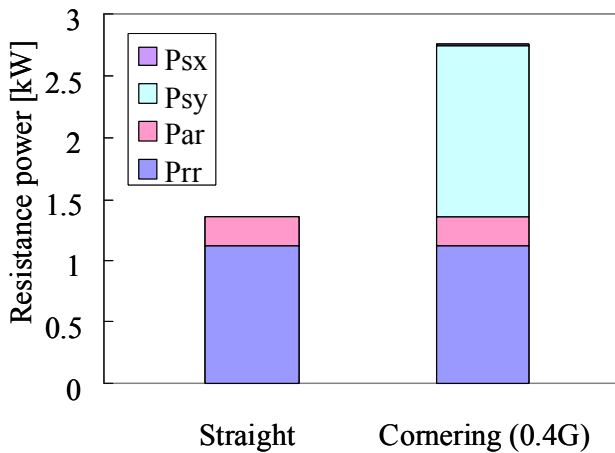


Figure 4: Comparison of resistance powers while driving straight and cornering ( $V = 30[\text{km/h}]$ ) by simulation

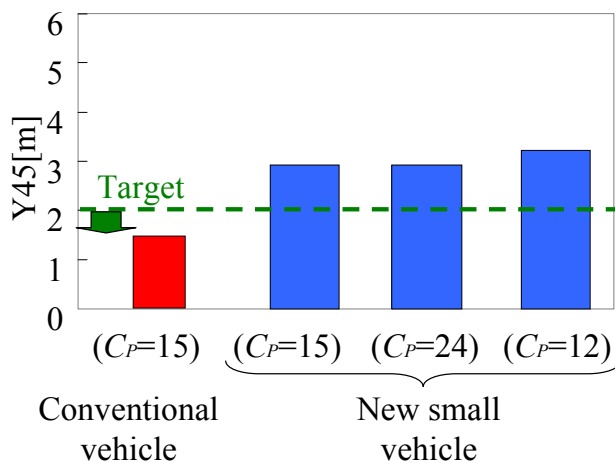


Figure 5: Simulation results of parameter study for stability against side wind between conventional vehicle and the new small vehicle

Figure 4 shows an example of a comparison of resistance powers between straight driving and cornering. It became clear that rolling resistance and cornering resistance were rather big and reducing those resistances was essential to reduce the power consumption. From equations (2), (4) and (5), it is understood that decreasing vehicle mass and tire RRC and also increasing tire cornering power (CP, normalized by tire contact load) are effective to reduce the total resistance power and improve the energy consumption of the vehicle. However, in general, decreasing RRC tends to result in decrease of CP for ordinary tires. Moreover, it is expected that decreasing vehicle mass

will result in reduced vehicle stability against external disturbances such as side wind. Figure 5 shows a result of parameter study for evaluating stability against side wind by Dymola. Evaluation criteria ( $Y45[\text{m}]$ ) in Figure 5 is the lateral deviation while driving at 120 km/h and pass a zone of 45m length with the side wind of 20m/s. In Figure 5, comparison between conventional vehicle ( $m = 1050[\text{kg}]$ ) and the new small vehicle ( $m = 600[\text{kg}]$ ) are shown. Also for the new small vehicle, some levels of normalized CP were researched. It became clear that the light-weight small vehicle is affected more than the conventional vehicle by side wind, and sensitivity of normalized CP value against the disturbance is very small. From above investigations it is indicated that developing new tire which can realize both low RRC and high CP value is necessary for reducing energy consumption. Also for coping with improving vehicle stability against external disturbances for such small vehicles, additional control of vehicle dynamics such as direct yaw moment control is considered to be necessary.

### 3 Development of necessary items to improve holistic performance of the new small vehicle

#### 3.1 New suspension system using tires with low RRC and high CP value

As mentioned in the previous section, the development of new tires for which both low RRC and high CP value can be realized will be necessary for reducing overall energy consumption. For this purpose, a new concept of tires called Large and Narrow (L&N) Concept was developed by Bridgestone [3]. It has characteristics of larger overall diameter, narrower section width and higher inflation air pressure than conventional tires. Figure 6 (cited from [3]) shows comparison of RRC and CP measurement data between ordinary reference tire, L&N tire and L&W (Large and Wide) tire representing current high performance tire. It can be seen that L&N tire has good balance of lower RRC and higher CP at high inflation pressure of 320 kPa. Thus, it was decided to adopt L&N tires for our new vehicle. Figure 7 shows a comparison of overall cornering resistance force ( $Cr$ ) calculated by the equation (6) when running on a constant radius corner at lateral acceleration of 0.4G.

Tire size	LI	OD [mm]	Category
175/65R15	84	608	Reference
205/50R18	89	660	Large & Wide
155/55R19	76	656	Large & Narrow

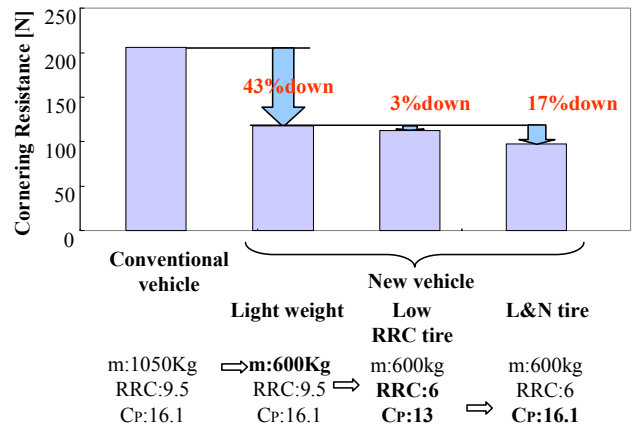



Figure 7: Comparison of cornering resistance force by simulation

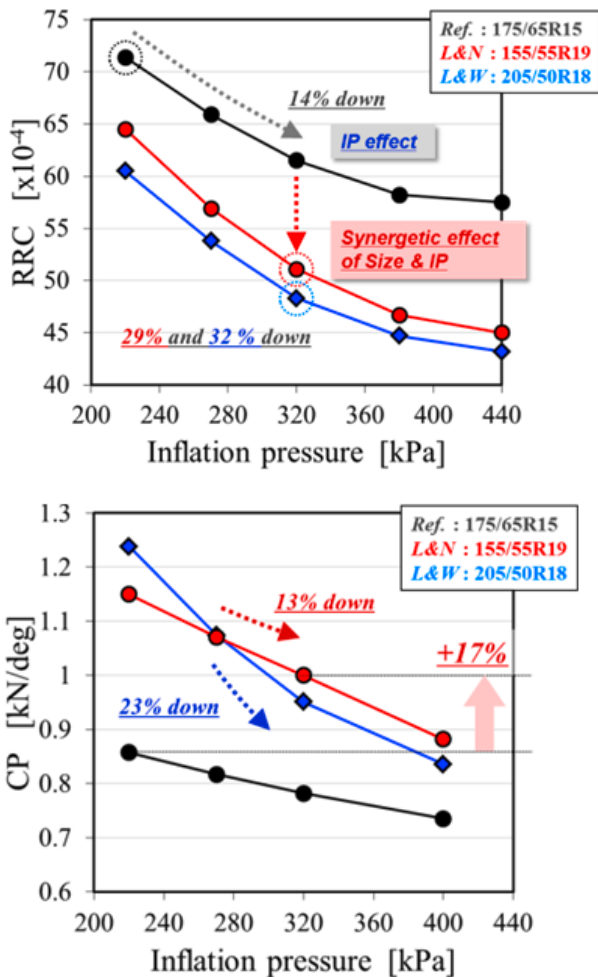


Figure 6: Measurement data of RRC and CP at Load=3.5kN [3]

$$Cr = mA_y^2 g / C_p \text{ [N]} \quad (6)$$

Comparison is done between conventional vehicle and new small vehicle with ordinary tire, low RRC (but low CP) tire and L&N tire. The effect of low weight and L&N tire to reduce the cornering resistance and thus energy consumption was proved by the simulation.

However, there still are remaining problems for applying L&N tires for the new vehicle. Because of larger overall size, it has larger rotating inertia resulting in larger drive-train vibration and less controllability of driving torque than conventional vehicle. Also higher inflation pressure results in higher vertical stiffness and it is suggested to affect ride comfort and NVH (Noise, Vibration and Harshness). Thus, new suspension design is supposed to be necessary. To cope with those problems are future works.

### 3.2 Active yaw moment control by torque vectoring system

As mentioned above, it became clear that active yaw moment control to cope with external disturbances was indispensable for small light-weight vehicles. To research the best solution of this function, benchmarking of existing torque vectoring systems were performed using simulation by Dymola at first. Considering the space for mounting and also controllability, TUM:MUTE type system[4] was investigated further. In this system, a main motor connected to outer ring gear of the differential planetary gear set controls total driving torque. On the other hand, a control motor connected with an input shaft of control gear sets controls torque distribution of left and right

wheel. The function of torque distribution was confirmed by Dymola simulation as shown in Figure 8. It became clear that torque distribution ratio can be changed from 50:50 to both of 0:100 and 100:0 and more by increasing the input torque of the control motor. By this simulation, also energy consumption of both main motor and control motor was able to calculate as well as mechanical transient motion. Finally an example of desired yaw rate feedback control for the torque distribution ratio was tested. Main motor torque ( $T_m$ ) was decided by PI feedback control of difference between desired value and actual value of the vehicle speed by following equation.

$$T_m = K_{pv} \cdot (V_{ref} - V) + K_{iv} \cdot \int (V_{ref} - V) dt \quad (7)$$

where

- $K_{pv}$ : Proportional feedback gain
- $K_{iv}$ : Integral feedback gain
- $V_{ref}$ : Desired vehicle speed
- $V$ : Actual vehicle speed

On the other, control motor torque ( $T_c$ ) was calculated by PI feedback control of difference between desired yaw rate and actual yaw rate as following equation.

$$T_c = K_{pr} \cdot (r_{ref} - r) + K_{ir} \cdot \int (r_{ref} - r) dt \quad (8)$$

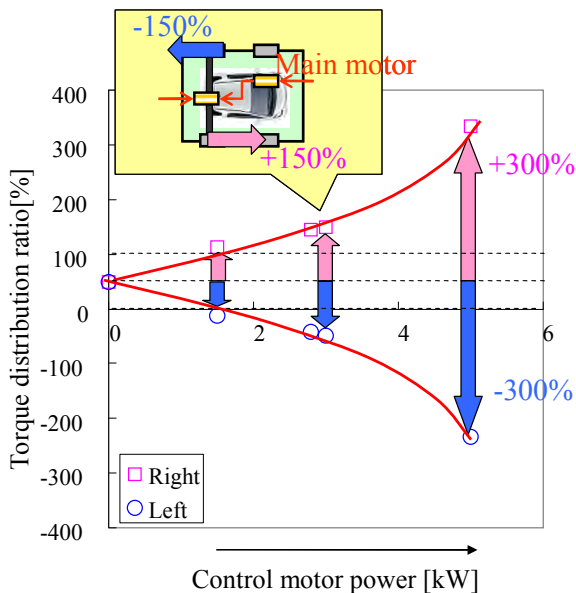


Figure 8: Simulation result of torque distribution ratio VS control motor power for torque vectoring differential gear system of MUTE type

where

- $K_{pr}$ : Proportional feedback gain
- $K_{ir}$ : Integral feedback gain
- $r_{ref}$ : Desired yaw rate
- $r$ : Actual yaw rate

and the desired yaw rate was calculated as below.

$$r_{ref} = \frac{K_s}{1 + sT_s} \delta_s \quad (9)$$

$$K_s = \frac{(a_f + a_r)c_f c_r V}{a_r c_r m V^2 + a_f (a_f + a_r)c_f c_r} \quad (10)$$

$$T_s = \frac{m a_f V}{(a_f + a_r)c_f} \quad (11)$$

Here,

- $\delta_s$ : Steering input angle at front tire
- $a_f$ : Longitudinal distance between front wheel and CG (Centre of gravity)
- $a_r$ : Longitudinal distance between rear wheel and CG
- $c_f$ : Cornering stiffness of front two tyres
- $c_r$ : Cornering stiffness of rear two tyres.

Figure 9 shows a simulation result of the side wind test. Lateral deviation against the side wind (Y45) and energy consumption of main motor and control motor were calculated for the cases of no control, only P feedback control and PI feedback control. The contradiction between vehicle stability and energy consumption of the control motor was confirmed. Finally, development of a new torque vectoring differential gear based on parallel planetary gear sets was decided. Numerical consideration as above will enable us to design the best solution for the practical design of the systems both in mechanical aspect and electrical aspect.

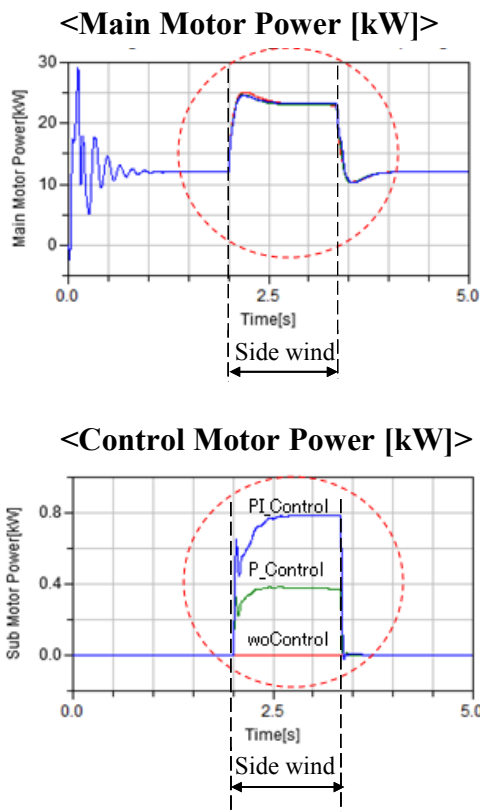
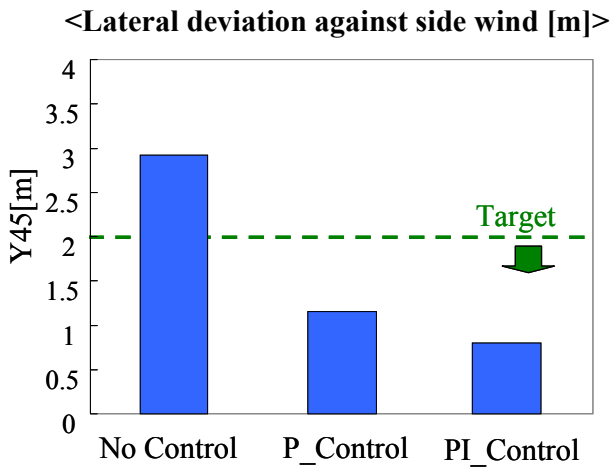


Figure 9: Simulation results of side wind test between No control, P feedback control and PI feedback control of torque vectoring differential gear

### 3.3 Electric regeneration system of braking force

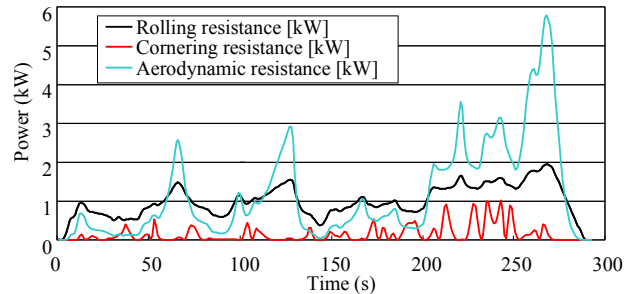


Figure 10: An example of calculation of each resistance power when driving on a winding circuit road

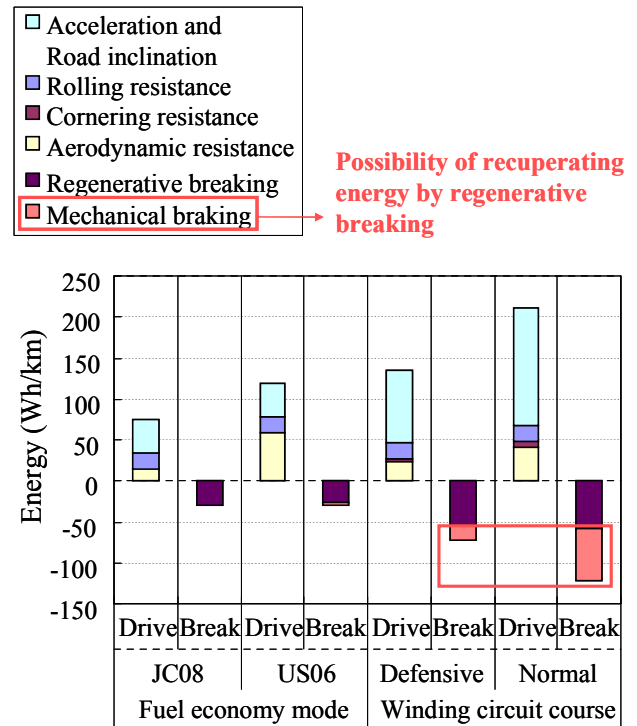


Figure 11: Comparison of driving and braking energy for some examples of driving modes

Utilizing electric regeneration of braking force by motor is effective to improve the energy consumption. In the planning phase of a new vehicle, it is necessary to decide proper size of battery capacity for the regeneration. For this purpose, realistic simulation of actual driving scenes is necessary. IPG CarMaker was used to calculate the vehicle speed, longitudinal and lateral acceleration, road decline and corner radius for actual roads. Using above data, necessary driving power and overall resistance power by the equation

(1) were calculated. Figure 10 shows an example of resistance power of each resistance force while driving on a winding circuit road. Using these results, overall driving energy and braking energy for some examples of driving mode were calculated as shown in Figure 11. Here, JC08 and US06 are regulation of driving modes for measuring fuel consumption in Japan and USA respectively. Figure 12 shows distribution of vehicle speed and longitudinal acceleration for both modes. As seen in Figure 12, US06 mode uses higher vehicle speed and acceleration than JC08 mode and results in more driving power and braking power appearing in Figure 11. Also in Figure 11, comparison of two driving styles for a winding circuit road is shown. It is observed that the defensive driving style needs less power than the normal driving style. It is assumed that braking power less than 15kW can be recuperated by the regeneration of motor in this example. It was understood that there is remained braking power which can be recuperated if the regeneration ability of battery system is large enough in the case of circuit road driving. In this example of Figure 11, these braking powers are consumed by the mechanical breaks and wasted. Figure 13 shows a result of simulation to calculate possible electricity consumption value in the cases of using battery systems whose regeneration ability are 15kW, 40kW and 70kW respectively. It became possible to estimate how large battery capacity was necessary to improve the energy consumption in each driving cases.

Consequently it was proved that these simulations were very useful to decide the proper specifications of a new vehicle in the planning phase.

## 4 Conclusions

For the investigation of overall vehicle specifications and system structures, a holistic vehicle model including mechanics, electrics, electronics, vehicle dynamics and control was made and utilized. It was proved that such a holistic model was very useful to investigate the proper specifications and system constructions in the phase of early stage of vehicle development. Modelica was very suited to make such a multi-discipline and multi-domain investigation by model-based development.

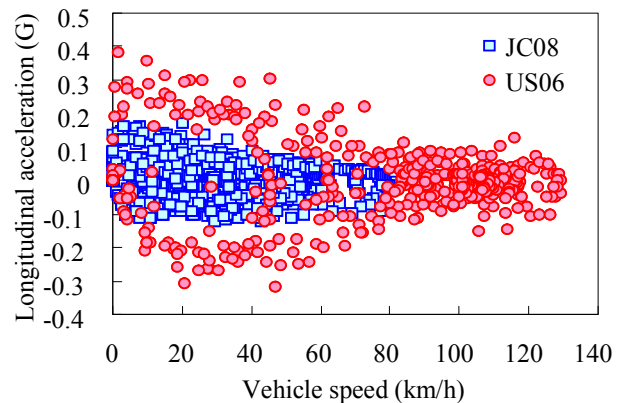


Figure 12: Vehicle speed VS longitudinal acceleration for JC08 and US06 modes

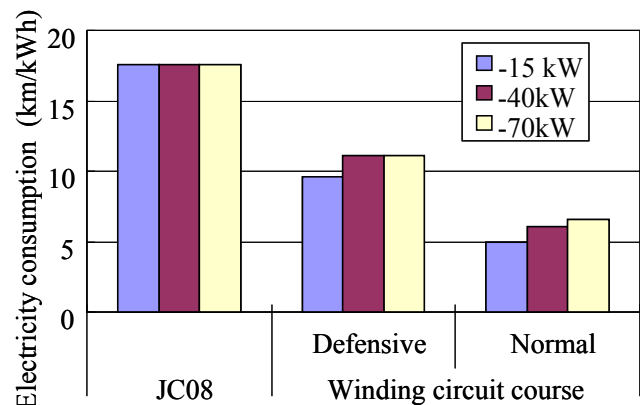


Figure 13: Comparison of estimated electricity consumption when changing the battery's ability of regeneration

## References

- [1] Informal document GRB-55-15 (55th GRB, 7-9 February 2012, agenda item 7(b)), European Commission, Enterprise and Industry
- [2] Kobayashi T., Katsuyama E., Sugiura G., Ono E., Yamamoto M.: "A research about driving force distribution control and energy consumption while cornering", Proceeding of 2013 JSAE Annual Congress (Spring), 352-20135393, 2013 (in Japanese)
- [3] Kuwayama I., Matsumoto H., Heguri H.: "Development of a next-generation-size tire for eco-friendly vehicles", Proceeding of

- Chassis.tech plus | 4th International Munich Chassis Symposium 2013, pp.623-644, 2013
- [4] Höhn B., Stahl K., Wirth C., Kurth F., Lienkamp M., Wiesbeck F.: “Electromechanical Power Train with Torque Vectoring for the Electric Vehicle MUTE of the TU München”, *Getriebe in Fahrzeugen 2011 Effizienzsteigerung im Antrieb*, 7./8./ Juni (2011), Friedrichshafen. VDI-Berichte Nr. 2130, 2011